Discover Applied Sciences

Review

The box-Behnken experimental approach of emerging contaminant-Ciprofloxacin antibiotic removal from aqueous solution using Kigelia Africana peel-activated carbon: optimization, kinetics, and isotherm studies

A. Annam Renita[1] · N. Magesh[2] · B. Senthil Rathi[3,4]

Received: 23 January 2024 / Accepted: 13 June 2024
Published online: 25 June 2024

Abstract
This study examined the use of Kigelia Africana peel-activated carbon (KAP-AC) to remove ciprofloxacin (CIP) from aqueous solutions. To investigate the adsorption capacity, isotherm, and kinetic parameters of the adsorption process, batch adsorption experiments were conducted to test the effects of adsorbent dosage, time, pH, initial concentration of CIP, and temperature. The binding mechanism among KAP-AC and CIP was investigated using FTIR, XRD, and SEM. Models of the Langmuir adsorption isotherm (LAI), Freundlich adsorption isotherm (FAI), and Temkin adsorption isotherm (TAI) helped to clarify the adsorption process. Adsorption experiments were carried out to explain kinetic studies, such as the pseudo-first-order kinetic model (PFO-KM), pseudo-second-order kinetic model (PSO-KM), and intraparticle diffusion kinetic model (IPD-KM). The experimental results may be more accurately described by the FAI and PFO-KM. Additionally, response surface methodology (RSM), which is based on Box–Behnken (BB) surface statistical design, was used to investigate the impact of variables on the adsorption of CIP. Higher coefficients of correlation and p-value values, by BB design, were in excellent adaption with the ideal combination of process variables, indicating the suitability of the selected model for assessing the experimental data.

Keywords Africana peel · Activated carbon · Ciprofloxacin removal · Emerging contaminant · Adsorption · Box–Behnken

Abbreviations

KAP-AC	Kigelia Africana peel-activated carbon
CIP	Ciprofloxacin
FTIR	Fourier Transform Infrared Spectroscopy
XRD	X-Ray diffraction
SEM	Scanning electron microscope
LAI	Langmuir adsorption isotherm
FAI	Freundlich adsorption isotherm
TAI	Temkin adsorption isotherm

✉ N. Magesh, mahya.mahesh@gmail.com; ✉ B. Senthil Rathi, rathisjce@gmail.com | [1]Department of Chemical Engineering, Sathyabama Institute of Science and Technology, Chennai, Tamil Nadu, India. [2]Department of Chemical Engineering, St Joseph's College of Engineering, Chennai, Tamil Nadu, India. [3]Department of Chemical Engineering, Sri Sivasubramaniya Nadar College of Engineering, Chennai 603 110, Tamil Nadu, India. [4]Centre of Excellence in Water Research (CEWAR), Sri Sivasubramaniya Nadar College of Engineering, Chennai 603 110, Tamil Nadu, India.

PFO-KM	Pseudo-first-order kinetic model
PSO-KM	Pseudo-second-order kinetic model
IPD-KM	Intraparticle diffusion kinetic model
RSM	Response surface methodology
BBD	Box–Behnken design
IC	Initial concentration
AD	Adsorbent dose
WWT	Wastewater treatment

1 Introduction

The quality of water resources has been completely degraded by population growth as well as the increasing production and consumption of newly developing contaminants. Both the quantity and variety of these dangerous contaminants, as well as the associated issues, are growing. In humans, they can result in enzymatic, hormonal, and genetic diseases. Numerous newly discovered contaminants have been documented in recent studies, and their metabolites have been found in aqueous media [1]. Pharmaceutical effluents containing antibiotics have lately drawn a lot of interest due to their possible side effects and the extensive usage of antibiotics. Antibiotic medication residues have grown to be a gravely neglected issue, even though the harm caused by antibiotics is not as obvious as that of other environmental pollutants [2].

Environmental antibiotic contamination poses a serious risk to human health worldwide. Among the latest generation of artificial fluoroquinolones, ciprofloxacin (CIP) is the most commonly used antibiotic globally [3]. Because CIP can remain in the surroundings, it has been extensively researched in aquatic environments. This contamination leaves behind residues in a variety of biological substrates as standard wastewater treatment (WWT) facilities are unable to eliminate it. This pollutant has been attenuated using a variety of cutting-edge WWT, but it is still reactive in surroundings [4, 5]. Photocatalysis [6, 7], advanced oxidation [8], biological degradation [9], and adsorption [10] are some of the methods used to degrade or remove antibiotics. Because of its outstanding efficacy and cost-effectiveness, adsorption is one of the most widely used techniques in developing nations [1]. As a result, there is a substantial rise in the use of inexpensive adsorbents derived from natural resources or waste from agriculture, with natural soils, mineral clays, and metal oxides drawing a lot of attention from scientific bodies [11, 12].

The adsorption efficacy of powdered AC magnetized by iron (III) oxide magnetic nanoparticles for the removal of CIP was thoroughly investigated. Using cutting-edge methods, iron (III) oxide magnetic nanoparticle-magnetized powdered AC was first created and manufactured by the co-precipitation method. It was then put through a characterization analysis. Subsequently, the iron (III) oxide magnetic nanoparticle-magnetized powdered AC's adsorption capacity for CIP was assessed at various initial CIP concentrations, pH values, amounts of powdered AC, shaking rates, contact times, and temperatures. At pH 7, dose = 1 g/L, agitation speed = 200 rpm, starting CIP concentration = 100 mg/L, interaction time = 60 min, and temperature = 298 K, the adsorbent demonstrated an outstanding adsorption capability for CIP 109.833 mg/g [13].

The innovative biomaterials made from banyan tree root systems via straightforward thermochemical treatment have a CIP capacity for adsorption. The ideal pH value of 8 and the appropriate absorbent dose of 0.03 g were discovered through the adsorption studies. The experiment's optimum capacity for adsorption was 99.27 mg/g, whereas the physically processed banyan root system showed a capacity for adsorption of 103.44% and a saturation adsorption capacity of 86.58 mg/g [14]. An environmentally acceptable agricultural waste called banana stem AC was made, and its ability to absorb the antibiotic CIP from the aqueous medium was studied [15]. CIP adsorption devices are made on *Prosopis juliflora* wood-derived acid AC. For CIP, the maximal Langmuir adsorption capacity was 250 mg/g [16].

To examine the adsorption characteristics of CIP on altered thermally activated kaolin, an integration of experimental and theoretical studies was conducted. CIP may be removed by adsorption up to 89.43% [17]. The adsorption of CIP in a static environment onto Verde-lodo bentonite clay that has been calcined. A maximum Langmuir removal capacity of 114.4 mg/g at 25 °C, and after heat treatment at 500 °C, clay showed significant reuse capacity. Clay's excellent removal capacity and regeneration potential make it a viable tactic to reduce newly developing pollutants found in wastewater [18]. A unique adsorbent for removing CIP from synthetic effluent was pistachio shell powder loaded with zinc oxide nanoparticles. More data fit the Langmuir isotherm model than the Freundlich model. The highest absorption of 129.1 mg/g was attained at pH 7, 100 mL of CIP solution, 0.1 g of adsorbent, 150 rpm, and 87 µm of particle size at 25 °C [19].

This study examined the use of KAP-AC as an adsorbent in the removal of CIP from aqueous solutions. Additionally, FTIR, XRD, and SEM analyses were carried out to elucidate the mechanism of interaction between KAP-AC and CIP. The effects of solution pH, contact duration, adsorbent quantity, and temperature factors were examined in adsorption studies. The models for Temkin, Freundlich, and Langmuir isotherms were employed to assess the results. Furthermore, kinetic models were established as a consequence of the data acquired. The impact of variables with solution pH, contact duration, the amount of adsorbent, temperature, and the starting concentration of CIP on achieving the maximum removal rate of CIP was examined using the Box-Behnken experimental design approach.

2 Materials and methods

2.1 Chemicals

Sigma Aldrich supplied analytical-quality ciprofloxacin (CIP) (≥ 98%) with MM of 331.34 g/mol and water solubility of 1.70 g/L, oleic acid (≥ 99%), and other reagent chemicals (≥ 98%). Working standards were followed in the dilution of the compounds. The properties of CIP are given in Table 1. By adding 0.05 N NaOH and 0.05 N HNO_3 to the stock solution, pH (AMAR digital and portable pH meter) is kept constant. African Kigelia fruit was gathered at Kanchipuram, Tamil Nadu. Double-distilled (DI) water was used to prepare the solution and all of the experimental methods.

2.2 Preparation of *Kigelia* Africana peel-activated carbon (KAP-AC)

The fruit's outer skin is painstakingly removed and sliced into tiny pieces. After being washed, the peel pieces were exposed to the sun to eliminate any remaining contaminants for a day. To eliminate the moisture content, the peels were placed in a hot air oven set at 110 °C for four hours. The adsorbent material is treated with oleic acid at a 1:2 ratio and mixed evenly for 24 h at 34 °C after the moisture content is removed. To prepare for activation, the chemically treated adsorbent material is dried and filtered. After that, the dehydrated fruit peel is heated to 400 °C for 45 min in a muffle furnace. The activated carbon was cleaned with a NaOH (0.05 N) solution to adjust the pH. The filtered activated carbon is once again stored in a hot air oven at 110 °C for 2 h after the pH has been adjusted. The produced activated carbon is gathered and packed in an airtight plastic bag once it has dried.

2.3 Characterization of *Kigelia* Africana peel-activated carbon (KAP-AC)

A variety of techniques were used to analyze the sample characterization. The field emission scanning electron microscope (FE-SEM) was employed to examine the surface morphology of KAP-AC. After being produced and dried, the adsorbent material was applied to the sample stub using an accelerating voltage of 20 kV. The Fourier-transform infrared (FTIR) spectrum was captured using a Perkin Elmer Spectra. It utilized the attenuated total reflectance approach for wavelengths of 400–4000 cm^{-1}. X-ray diffraction (XRD) was employed to analyze the structural and crystal phase of the adsorbent material, using a high-performance diffractometer operating at 40 kV and 40 mA. A scanning rate of 2° min^{-1} was used to set the angle 2θ between 3° and 80°.

Table 1 Properties of CIP

Property	Values
Chemical formula	$C_{17}H_{18}FN_3O_3$
Molecular weight	331.34 g/mol
Low K_{ow} a	0.28
Water solubility	1.70 g/L
Biological half life	3.5 h

Table 2 Different types of isotherms used Ciprofloxacin removal by KA-MAC

	LAI	FAI	TAI
Equation	$q_e = \frac{C_e K_L q_m}{1+C_e K_L}$	$q_e = K_F C_e^{1/n}$	$q_e = \frac{RT}{b_t} \ln(a_t c_e)$
Parameters	q_m (mg/g)-maximum chemisorption capacity at the saturation system, K_L (L/mg).-Langmuir constant value	K_F ((mg/g) (L/mg)$^{1/n}$)-reundlich constant value n-Freundlich exponential	K, b_t and a_t-isotherm constants
Reference	[20]	[21]	[22]

Table 3 Different types of kinetics used Ciprofloxacin removal by KA-MAC

	PFO-KM	PSO-KM	IPD-KM
Equation	$q_t = q_e(1 - e^{-k_1 t})$	$q_t = \frac{q_e^2 k_2 t}{1+q_e k_2 t}$	$q_t = C + K_3 t^{0.5}$
Parameters	K_1 (1/min)-First order sorption rate constant	K_2 g. (mg min)$^{-1}$-second order sorption rate constant	K_3 (mg g^{-1} min$^{-0.5}$)-intraparticle diffusion rate constant of the kinetic model
References	[23]	[24]	[25]

2.4 Adsorption studies

The effects of temperature (45° to 75 °C), contact duration (20–120 min), solution pH (2–10), and solid/liquid ratio of KAP-AC (2.5–5 g/L) on CIP adsorption were studied using an initial concentration (IC) of CIP solution (50–120 mg/L). In all adsorption experiments, 100 ml of CIP solution were introduced to 150-ml Erlenmeyer flasks. The CIP-KAP-AC solution was shaken at 120 rpm for 120 min. To assess the impact of solution pH, 0.05 N HNO_3 or 0.05 N NaOH solution was added, and shaking solutions with pH adjustments were performed until the system reached equilibrium. The starting and final concentrations (FC) of CIP left in the solutions were determined using a UV–visible spectrophotometer (JASCO-V670) set to maximum absorbance at λmax = 276 nm. The adsorption and removal capacities were computed using the following equations.

$$\%\ \text{CIP removal} = \frac{(C_O) - (C_e)}{(C_O)} \times 100 \tag{1}$$

$$q_e = \frac{(C_0 - C_e)}{W} \times V \tag{2}$$

where, C_O–IC of CIP (mg/L), Ce–FC of CIP (mg/L), w- mass of KAP-AC (g), V- volume of solution (mL), q_e- quantity of CIP uptake on unit mass basis of the KAP-AC under equilibrium conditions (mg/g).

2.5 Adsorption isotherm

100 mL of a 40–200 mg/L CIP solution was stirred with KAP–AC at 120 rpm to find the adsorption isotherms. Various isotherm models, including LAI, FAI, and TAI, were employed to elucidate adsorption investigations and identify isotherm behavior. The formulas in Table 2 can be used to calculate these models. FAI acknowledges that multiple-layer adsorption takes place on the adsorbent, but LAI only recognizes single-layer adsorption. In contrast to a logarithmic decline in adsorption heat, TAI is expected to have a linear drop.

2.6 Adsorption kinetics

100 mL of a 40–200 mg/L CIP solution was stirred with KAP–AC at 120 rpm to find the adsorption kinetics. The mechanism behind the adsorption procedures and adsorption behavior is explained by adsorption kinetics. Adsorption tests

Table 4 Independent variables for Box Behnken Design and its level

Coded value	Unit	Low (–1)	High (+ 1)
A (pH)	–	2	12
B (IC of CIP)	ppm	40	200
C (Time)	min	20	120
D (Temperature)	◦C	45	85
E (Adsorbent dose)	g/L	1	5

Fig. 1 FTIR image of KAP-AC

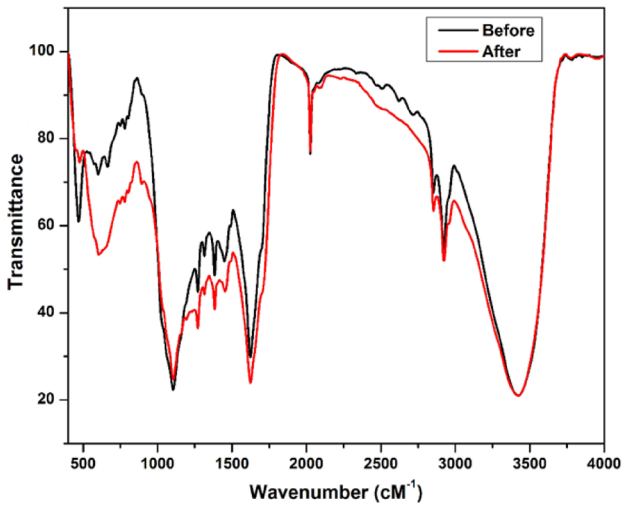

were conducted using PFO-KM, PSO-KM, and IPD-KM at various concentrations to explain the kinetic investigations. The formulas in Table 3 can be used to calculate these models.

2.7 Box-Behnken experimental design

Response surface methodology (RSM) is an effective combination of statistical and mathematical methods for process optimization, which makes it appropriate for investigating both the complex and relative interactions between different components [26]. CIP elimination was optimized using a factorial trial methodology. Box Behnken Design (BBD), one of the few RSM design techniques, to examine the distinct and intricate effects of process factors on CIP removal was used [27]. The optimal performance for a response surface methodology issue with five components is achieved by the BBD. Adsorbent dosage, pH, CIP's IC, time, and temperature were selected as the study's variables. The variables included three levels: high (1), low (– 1), and the following factors: A (pH), B (IC of CIP), C (time), D (temperature), and E (adsorbent dosage). The temperature, pH, time, IC of CIP, and amount of adsorbent were chosen as the independent factors, while the effectiveness of CIP removal (%) was the response variable. A detailed summary of the independent variables for CIP elimination, together with their respective experimental ranges and three levels, is given in Table 4. To perform the BBD, we used Stat-Ease software (Design-Expert 13.0) to run 46 tests, containing 6 centered points.

3 Results and discussion

3.1 Characterization of *Kigelia* Africana peel-activated carbon (KAP-AC)

It was observed that several functional groups present on the surface of KAP-AC were elucidated using FTIR analysis. Figure 1 shows the FTIR spectra of the KAP-AC adsorbent material. The spectra of KAP-AC are analyzed within the wavelength range between 400 and 4000 cm^{-1}. From the spectrum-impinged figure, peaks were observed in the range of 599 cm^{1}, indicating the presence of the C–I alkyl halides group. The spectra obtained at 1098 cm^{-1} attribute the presence of cellulose and lignin. This was observed because of the use of alcohol in cleaning the adsorbent material. Peaks

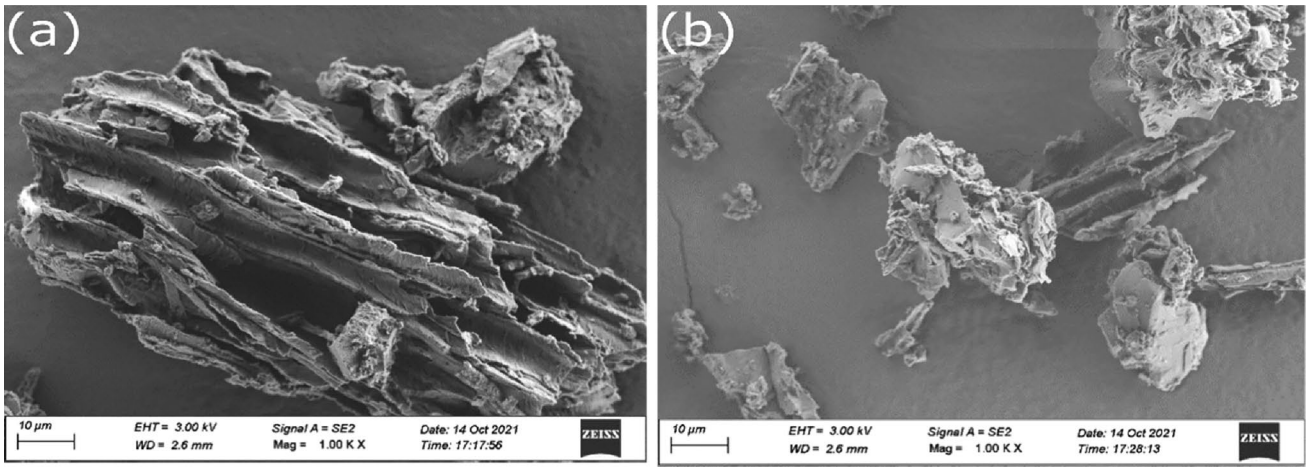

Fig. 2 **a** FESEM image of KAP-AC before adsorption; **b** FESEM image of KAP-AC after adsorption

Fig. 3 XRD analysis of KAP-AC

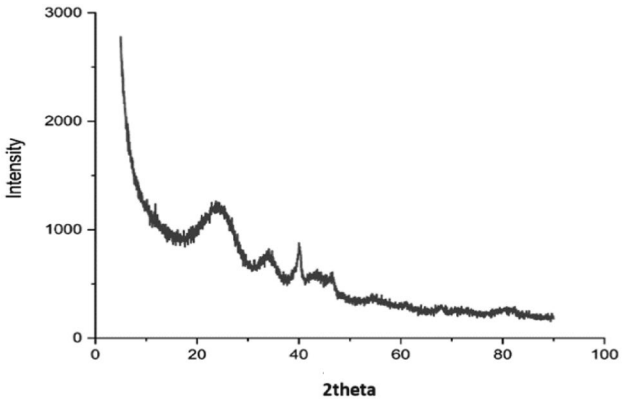

are observed between 1098 and 1621 cm^{-1}, representing the C = C aromatic groups. The next peak was observed at the wavelength of 1621 cm^{-1}, indicating the C = O lignin group. The adsorption peak at 2024 cm^{-1} is associated with the presence of C≡C alkyne group. The broad streak peak at 2918 cm^{-1} and 3399 cm^{-1} corresponds to C-H and OH stretch of cellulose and alcohol. This was observed because of the use of alcohol in cleaning the adsorbent material. The adsorption band observed at 3744 cm^{-1} was assigned to be water.

The FESEM analysis of KAP-AC is displayed in Fig. 2a, b. According to the figure, the adsorbent material was enhanced by treating it with oleic acid, as evidenced by the crumbly cell structure and uneven diameter of the material. Figure 2a clearly illustrates the many void cells found on the adsorbent surface, suggesting good adsorption outcomes. At 400 °C, these pores are activated, increasing their size. More porosity makes it easier for CIP molecules to adsorb and get occupied in them. It can be seen from Fig. 2b that fewer holes exist as a result of the CIP molecule adhering to the surface following treatment.

The diffractogram radiation images created when KAP-AC was exposed were used to analyze the adsorbent material's composition. The pattern of KAP-AC adsorbent material impregnated with oleic acid is seen in Fig. 3. Determining the adsorbent material's phase diagnosis and crystal structure is the goal of XRD analysis. The XRD data show that while KAP-AC contains few contaminants, it was also discovered to have unwanted peaks. The pattern suggests that the KAP-AC adsorbent material is amorphous in nature based on the observed peaks at 2θ values.

3.2 Solution pH impact on CIP removal

A significant aspect affecting the adsorption process is the pH of the solution; Fig. 4 shows how this affects the adsorption of CIP ions onto KAP-AC. The pH of the KAP-AC with zero charge is found to be 4. It appears that an increase in pH was accompanied by an increase in the absorption of CIP ions by the KAP-AC, which peaked at pH 4 and then abruptly

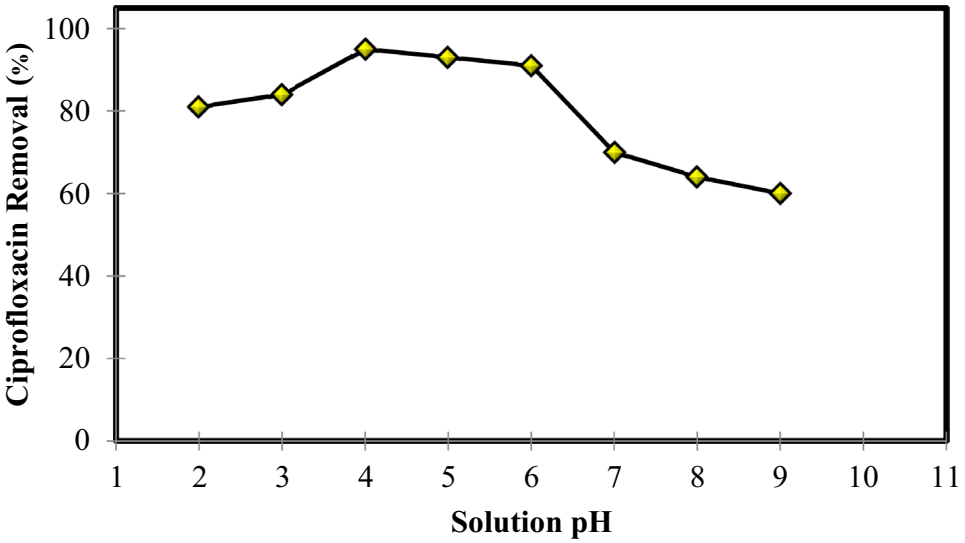

Fig. 4 Effect of pH on Ciprofloxacin removal by KAP-AC (KAP-AC Dose = 5 g/L; Contact time = 2 h; Temperature = 85 °C; IC of Ciprofloxacin = 40 ppm)

fell above it to maintain a pH of 5. CIP occurs as a distinct species based on the pH of the solution; this species range has been investigated in the literature [28]. One explanation for the impact of solution pH is the electrostatic contact force that adsorbents propagate. Columbia repulsion force arises because of like charges when the pH is less than 2–3, and the surface of the adsorbent and predominant ions in the medium are both positive. Thus, decreased adsorption occurs because the affinity of the CIP ions for the binding sites on the KAP-AC is slow [28]. Perhaps the positive CIP ions attach to the more negatively charged surface of KAP-AC when the pH rises (becomes less acidic). Additionally, the adsorbents may have active areas where ion exchange can occur. CIP ion molecules may have aggregated more quickly to form dimers above pH 4. This might be due to zwitterion effects.

A coexisting liquid bulk phase's pH level may have an impact on the KAP-AC's surface potential. Zero charge point (PZC) is the pH value at which there is no surface charge. When pH is less than pH_{PZC}, the surface will be positively charged, whereas when pH is greater than pH_{PZC}, it will be negatively charged. With a pH_{PZC} of 5.8, the KAP-AC surface will always be positively charged at pH values below pH_{ZPC} and negatively charged at pH values greater than pHpzc [33].

3.3 KAP-AC dose impact on CIP removal

The impact of KAP-AC dose on CIP adsorption was investigated by shaking a 100 mL 40 ppm CIP solution for 2 h at 85 °C. A range of KAP-AC concentrations (1–5 g/L) were employed to investigate how adsorbent dose affected adsorption capability. Figure 5 illustrates how an increase in KAP-AC led to a rise in CIP adsorption from 60.54% to 94.2%. The highest adsorption of 1 g/L KAP-AC achieved 94.2% adsorption, owing to the obtained data, and a 1 g/L solid/liquid ratio was employed for all adsorption investigations. Figure 5 shows that when the amount of KAP-AC increased, the adsorption capacity dropped. The covering of sites for adsorption by CIP molecules explained this

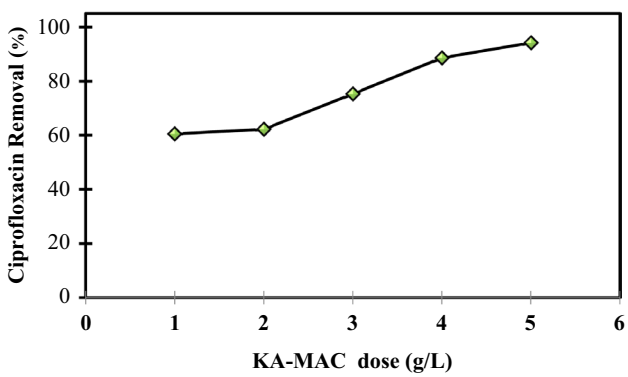

Fig. 5 Effect of adsorbent dose on Ciprofloxacin removal by KAP-AC (pH = 4; Contact time = 2 h; Temperature = 85 °C; IC of Ciprofloxacin = 40 ppm)

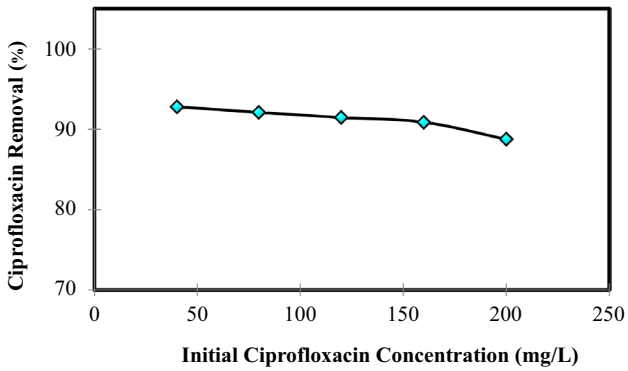

Fig. 6 Effect of IC of Ciprofloxacin on removal by KAP-AC (pH = 4; Contact time = 2 h; Temperature = 85 °C; KAP-AC Dose = 5 g/L)

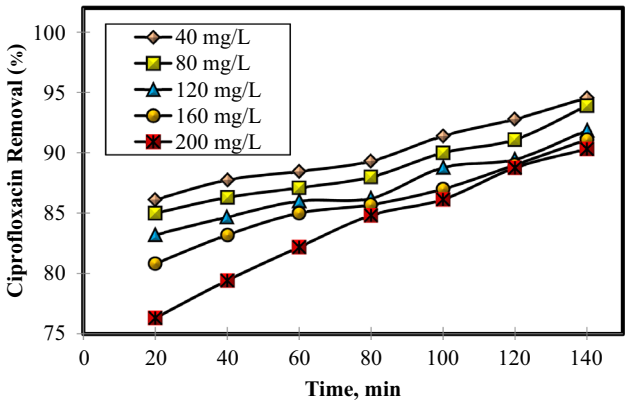

Fig. 7 Effect of contact time on Ciprofloxacin removal by KAP-AC (pH = 4; IC of Ciprofloxacin = 40 ppm; Temperature = 85 °C; KAP-AC Dose = 5 g/L)

decline. At large adsorbent doses, the interchangeable sites across the adsorbent could not be completely covered by existing CIP molecules. As a result, when the amount of KAP-AC increased, the adsorption capacity decreased.

3.4 IC of CIP impact on CIP removal

As the IC of CIP grew from 40 to 200 mg/L, Fig. 6 demonstrated that the removal (%) of CIP dropped. Under the specified testing circumstances, the KAP-AC composites' maximum CIP adsorption capacity could be 73.71 mg/g. Less removal (%) at higher dye concentrations was seen at higher MB concentrations because a larger driving force was required to overcome the mass transfer barrier for CIP molecules between the aqueous phase and solid phase. KAP-AC compounds could only adsorb a portion of the CIP molecules because there is a limit to the number of adsorption sites for a particular KAP-AC dose. Because of this, the removal (%) of CIP was higher at lower IC of CIP values but decreased at higher IC of CIP values.

3.5 Contact time impact on CIP removal

When adsorption is finished and the adsorbent is unable to hold any more material on its surface, that is the right contact time to utilize in CIP adsorption studies. The impact of contact duration on CIP adsorption was investigated by shaking 100 mL of CIP solution containing 40–200 ppm and 5 g/L KAP-AC for two hours at 85 ℃. Figure 7 shows that roughly 92.8% of CIP was removed in two hours at 40 ppm of CIP and that CIP adsorption did not alter much after that point. Because of this, two hours was decided upon as the proper contact period, and this duration was maintained throughout the trials. These active sites were gradually occupied throughout the course of the adsorption, which led to a decrease in the effectiveness of the adsorption process because there were fewer effective interactions between the dye molecules and the adsorbent.

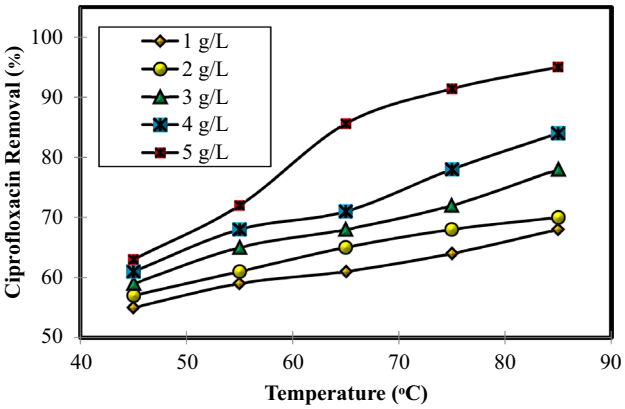

Fig. 8 Effect of temperature on Ciprofloxacin removal by KAP-AC (pH = 4; IC of Ciprofloxacin = 40 ppm; Contact time = 2 h; KAP-AC Dose = 5 g/L)

Table 5 Isotherm analysis on the Ciprofloxacin removal by KA-MAC

Models	Parameters	Ciprofloxacin removal
Langmuir	q_m (mg/g)	73.71
	K_L (L/mg)	0.048
	R^2	0.988
Freundlich	K_F [(mg/g)(L/mg)$^{(1/n)}$]	4.776
	n	1.466
	R^2	0.996
Temkin	A (L/mg)	0.737
	B	12.58
	b (kJ/mol)	0.236
	R^2	0.95019

3.6 Temperature impact on CIP removal

The connection between temperature and the IC of the CIP ions adsorbed onto the KAP-AC at two hours is described by the influence of temperature parameters on the uptake of CIP ions by KAP-AC. The adsorption of the CIP ions on the KAP-AC increased as the temperature rose from 45 to 85 °C, as shown in Fig. 8. The rise in CIP ion adsorption may be due to an increase in the ions' mobility brought on by the system's energy acquisition. This suggested that the CIP ion-active site interaction at the KAP-AC surface is an endothermic reaction, which is analogous to a chemical adsorption process.

3.7 Adsorption isotherms

Using the LAI, FAI, and TAI, the adsorption data of CIP on KAP-AC were analyzed. The findings are displayed in Table 5, and plots are displayed in Fig. 9. The poor correlation coefficient suggests that LAI did not adequately explain the adsorption mechanism of CIP onto KAP-AC. Furthermore, the observed adsorption value and the predicted adsorption capacity were far off. The FAI model's R^2 value of 0.996 indicated that it was a better fit for explaining the adsorption process of CIP onto KAP-AC. This finding demonstrated that CIP was adsorbed in many layers at non-uniform binding sites during its adsorption on KAP-AC. The energetically heterogeneous surface was produced via KAP-AC. Furthermore, KAP-AC has unique qualities such a porous structure and a wide surface area. Hence, many methods may have been implicated when KAP-AC substance was adsorbed CIP.

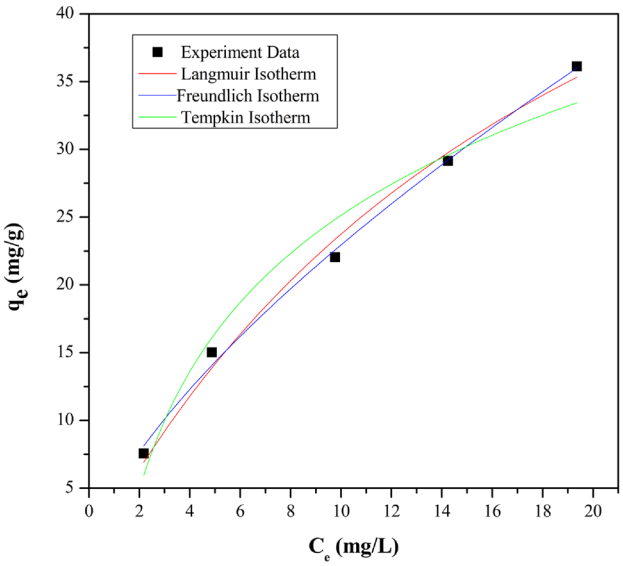

Fig. 9 Adsorption isotherms on the Ciprofloxacin removal by KAP-AC

3.8 Adsorption kinetics

When comparing the coefficients of correlation of the kinetic equations at various temperatures, the PFO-KM more closely matched the system at all concentrations than the other kinetic models. At 40, 80, 120, 160, and 200 ppm IC

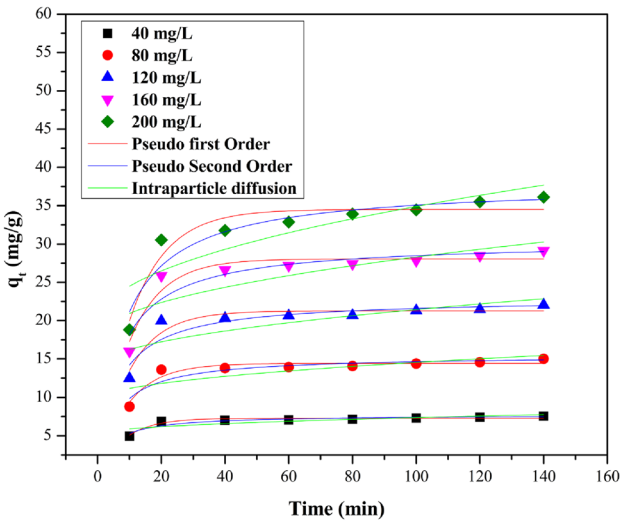

Fig. 10 Adsorption kinetics on the Ciprofloxacin removal by KAP-AC

Table 6 Kinetic studies on Ciprofloxacin removal by KA-MAC

Models	Parameters	Concentration (mg/L)				
		40	80	120	160	200
PFO-KM	k_1 (min^{-1})	0.11976	0.10502	0.10039	0.09559	0.08643
	$q_{e,}$ cal (mg/g)	7.29299	14.42179	21.27515	28.05661	34.51979
	R^2	0.92928	0.90959	0.91036	0.91958	0.92067
PSO-KM	k_2 (g/mg. min)	0.02852	0.01137	0.00713	0.00496	0.00336
	$q_{e,}$ cal (mg/g)	7.73181	15.46851	22.91122	30.37076	37.83232
	R^2	0.86869	0.83136	0.82782	0.85146	0.90215
IPD-KM	k_p	0.21409	0.49473	0.76379	1.07467	1.52258
	C	5.22649	9.60507	13.81041	17.55081	19.67475
	R^2	0.58723	0.54164	0.52973	0.56535	0.67289

of CIP, respectively, the correlation coefficients of PFO-KM were determined to be 0.92928, 0.90959, 0.91036, 0.91958, and 0.92067. The PFO-KM was used to compute the qe value, which at 34 mg/g at 200 ppm was the experimental qe value. The two results that were obtained agreed with one another. It was determined that other stages may be rate-determining steps since PFO-KM suited CIP adsorption in the presence of KAP-AC the best. Therefore, the particle diffusion kinetic model was not a rate-determining step. In addition, a rise in adsorption capacity and a drop in the rate constant were brought on by an increase in concentration values. Figure 10 displays the kinetic data that were derived using kinetics models and are provided in Table 6.

3.9 Desorption and reusability

Figure 11 illustrates how the removal of CIP on KAP-AC might reach 95.03% in the first cycle and sustain a removal percentage of 60.5% in the fifth cycle. The coverage of the adsorbed CIP on the KAP-AC material surface may be the cause of the reduction in the adsorption quantity. In conclusion, KAP-AC demonstrated a high adsorption capacity and was found to be reusable.

3.10 Box-Behnken design and 3-D RSM

By examining the potential interactions among the factors under study and their impact on CIP adsorption, the Box-Behnken Design (BBD) was utilized to maximize the number of tests required. The BBD design is globular and rotating, with a cube's center point confined to a sphere [29]. It has been employed to optimize various physical and chemical processes, with the number of tests chosen in line with specific research goals [30].

This study employed a two-level factorial BBD to investigate and validate adsorption factors influencing the removal of CIP onto KAP-AC. The variable parameters included KAP-AC dosage (1–5 g/L), pH (2–12), initial concentration (IC) of CIP (40–200 ppm), duration (20–120 min), and temperature (45–85 °C). The factor levels were encoded as 1 (high) and – 1 (low). The experimental design levels and input parameters are detailed in Table 4.

In this investigation, a Box-Behnken Design (BBD) was employed, consisting of 46 tests to assess the effects of these characteristics both separately and in combination. The experimental settings for pH, temperature, time, CIP's IC, and adsorbent amount are presented in Table 7, along with the observed removal efficiency. A second-order model was employed to illustrate the mathematical relationship between the response values and the independent process variables, utilizing the experimental data from Table 7. Equation (3) represents the model depicting the elimination effectiveness concerning pH (A), IC of CIP (B), time (C), temperature (D), and KAP-AC dose (E).

$$\begin{aligned}\text{Removal of CIP} \;=\; &+42.51 - 28.64\,A - 3.05\,B + 3.90\,C + 9.03\,D + 10.81\,E - 0.1405\,BC \\ &+ 6.18\,DE + 6.87\,A^2 + 1.14\,B^2 + 0.2560\,C^2 - 3.97\,D^2 + 2.13\,E^2\end{aligned} \tag{3}$$

The statistical significance of the ratio of mean square variation due to regression and mean square residual error was determined using analysis of variance, often known as ANOVA [31]. ANOVA is a statistical approach that, to test hypotheses regarding the model's parameters, splits the overall variance in the data into component portions associated with specific sources of variation [32]. P-values were employed to assess the significance of the KAP-AC dose, pH, time, CIP's initial concentration (IC), and temperature interactions. Table 8 provides the ANOVA results for the response

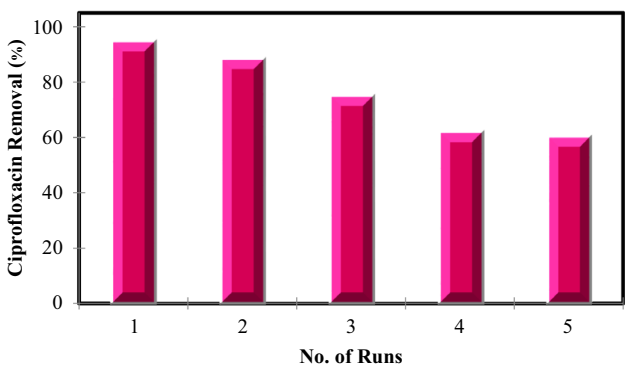

Fig. 11 Desorption studies on the Ciprofloxacin removal by KAP-AC

Table 7 The experiment parameters for pH, temperature, time, IC of CIP and adsorbent quantity as well as the observed removal efficiency findings

Run	Factor 1 A: pH	Factor 2 B: IC of CIP ppm	Factor 3 C: Time min	Factor 4 D: Temperature ℃	Factor 5 E: Dose g/L	Response 1 Removal of CIP %
1	4	40	120	85	5	95.03
2	4	40	120	85	5	95.03
3	4	40	120	85	5	95
4	4	40	140	85	5	94.56
5	4	80	140	85	5	93.9
6	5	40	120	85	5	93
7	4	40	120	85	5	92.8
8	4	40	120	85	5	92.8
9	4	80	120	85	5	92.1
10	4	120	140	85	5	91.86
11	4	120	120	85	5	91.46
12	4	40	120	75	5	91.4
13	4	40	100	85	5	91.4
14	4	80	120	85	5	91.1
15	4	160	140	85	5	91.1
16	6	40	120	85	5	91
17	4	160	120	85	5	90.88
18	4	200	140	85	5	90.32
19	4	80	100	85	5	90
20	4	80	60	85	5	87.1
21	4	160	100	85	5	87
22	4	80	40	85	5	86.3
23	4	120	80	85	5	86.24
24	4	200	100	85	5	86.14
25	4	40	20	85	5	86.12
26	4	120	60	85	5	86
27	4	160	80	85	5	85.7
28	4	40	120	65	5	85.6
29	4	80	20	85	5	85
30	4	160	60	85	5	85
31	4	200	80	85	5	84.82
32	4	40	120	55	4	68
33	4	40	120	65	2	65
34	4	40	120	55	3	65
35	8	40	120	85	5	64
36	4	40	120	75	1	64
37	4	40	120	45	5	63
38	4	40	120	65	1	61
39	4	40	120	55	2	61
40	4	40	120	45	4	61
41	9	40	120	85	5	60
42	4	40	120	55	1	59
43	4	40	120	45	3	59
44	11	40	120	85	5	58
45	4	40	120	45	2	57
46	12	40	120	85	5	55

Table 8 ANOVA quadratic response for removal of CIP

Source	Sum of squares	df	Mean Square	F-value	p-value
Model	8531.27	12	710.94	102.95	< 0.0001
A-pH	2747.80	1	2747.80	397.92	< 0.0001
B-IC of CIP	28.80	1	28.80	4.17	0.0492
C-Time	48.15	1	48.15	6.97	0.0125
D-Temperature	217.70	1	217.70	31.53	< 0.0001
E-Dose	760.64	1	760.64	110.15	< 0.0001
BC	0.0520	1	0.0520	0.0075	0.9314
DE	93.47	1	93.47	13.54	0.0008
A^2	28.61	1	28.61	4.14	0.0499
B^2	5.28	1	5.28	0.7653	0.3880
C^2	0.2487	1	0.2487	0.0360	0.8506
D^2	32.31	1	32.31	4.68	0.0379
E^2	6.79	1	6.79	0.9830	0.3287
Residual	227.88	33	6.91		
Lack of fit	221.46	28	7.91	6.17	0.0257
Pure error	6.41	5	1.28		
Cor. Total	8759.15	45			

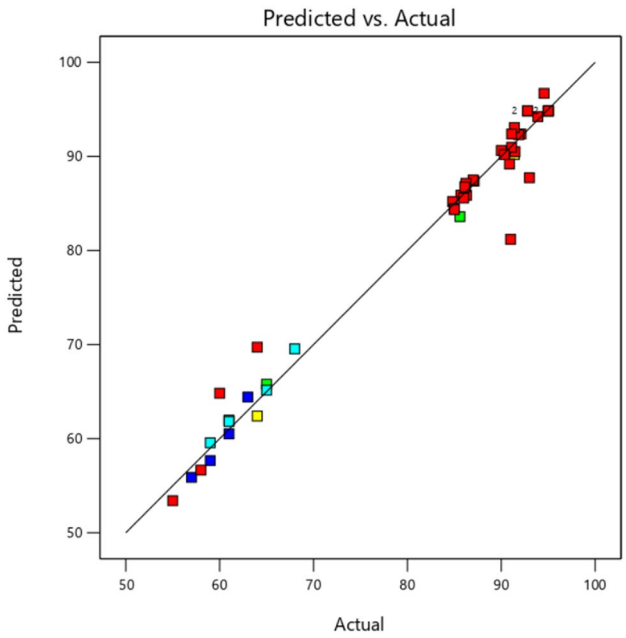

Fig. 12 Actual Response vs Predicted response

surface quadratic model. The model was considered significant based on its F-value of 102.95. An F-value of this magnitude had only a 0.01% probability of being the result of noise. Model terms are deemed significant when P-values are less than 0.0500. In this instance, A, B, C, D, E, DE, A^2, and D^2 are important model terms. Model terms are considered not important if their P-values exceed 0.1000. If a model has many unimportant terms (except those needed to maintain hierarchy), model reduction may improve its performance. The quadratic model produced a determination coefficient (R^2) of 0.974 and an adjusted determination coefficient (R^2 Adj) of 0.9645, indicating high significance and strong fitness for the statistical model. The relationship between expected and actual response values was clarified in Fig. 12, with the cluster points surrounding the diagonal line demonstrating a successful model fit.

To assess the primary and interaction impacts of two factors, three-dimensional response surface plots were generated as a function of two factors at a time, while keeping all other components at fixed values. The model used one dependent variable, the percentage of CIP removed, and five independent variables: pH, time, temperature, IC of CIP, and KAP-AC

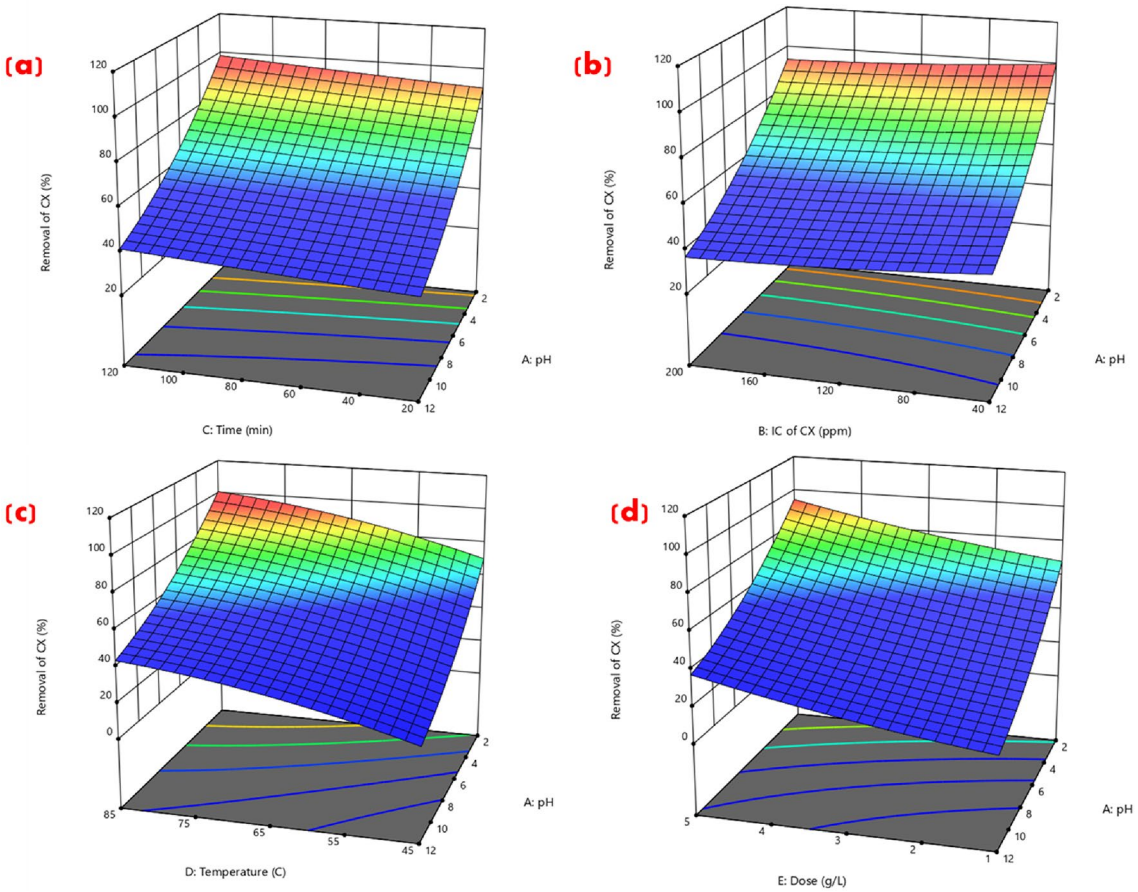

Fig. 13 3-D plot for the removal of CS along with pH and **a** time; **b** IC of CIP; **c** Temperature; **d** KAP-AC dose

dosage. Three-dimensional response surface plots for CIP removal are presented in Fig. 13. These plots exhibited signs of nonlinearity, indicating strong interactions between variables and adsorption capacity. Figure 13a displayed the effects of time and pH, revealing that the maximum elimination occurred at the highest time and lowest pH value. Similarly, Fig. 13b shows the impacts of pH and CIP's IC, with the greatest elimination observed at the lowest pH and IC of CIP values. Figure 13c and d illustrate the effects of temperature and KAP-AC dosage on pH, respectively.

4 Conclusion

The present study utilized KAP-AC, an affordable adsorbent, for the removal of CIP from aqueous solutions. The activated carbon prepared from Kigelia Africana peel treated under oleic acid is characterized and applied for the adsorption of Ciprofloxacin. The activated carbon is prepared at 400 °C to provide maximum active sites in the adsorbent material for greater adsorption. From the adsorption studies, it is understood that maximum adsorption of CIP is obtained at a pH range of 4.0 with the adsorbent dosage of 5.0 g/L of KAP-AC material to the contact time of 120 min at a temperature of 85 °C. Employing Box-Behnken Design (BBD), the study investigated the effects of temperature, time, initial concentration of CIP (IC), KAP-AC dosage, and pH on removal efficiency. Through Response Surface Methodology (RSM) via BBD, it was identified that five independent factors—KAP-AC dosage, pH, time, IC of CIP, and temperature—significantly influenced the dependent variable, namely, the percentage elimination of CIP. The quadratic model was found to suit the experimental data well, as indicated by the p values obtained from the lack-of-fit test.

Isotherm results for KAP-AC CIP removal demonstrated a good fit with the Freundlich Adsorption Isotherm (FAI). Additionally, adsorption kinetic experiments revealed that the kinetics of CIP followed the Pseudo-First-Order Kinetic Model (PFO-KM). In summary, the study's findings strongly suggest that KAP-AC holds significant promise as an

innovative, efficient, and cost-effective alternative adsorbent for the removal of pharmaceuticals and other environmental contaminants.

Author contributions All authors contributed to the study conception and design. Material preparation, Experiments and article data collection and draft was performed by Magesh N. The main manuscript text, modelling, prepared figures and tables were written by B Senthil Rathi and all authors commented on previous versions of the manuscript. Supervision by Annam Renita A. All authors read and approved the final manuscript.

Data availability Data available on request.

Declarations

Competing interests The authors declare that no competing interests in this research article.

References

1. Malakootian M, Faraji M, Malakootian M, Nozari M, Malakootian M. Ciprofloxacin removal from aqueous media by adsorption process: a systematic review and meta-analysis. Desalin Water Treat. 2021;229:252–82.
2. Yu F, Sun S, Han S, Zheng J, Ma J. Adsorption removal of ciprofloxacin by multi-walled carbon nanotubes with different oxygen contents from aqueous solutions. Chem Eng J. 2016;285:588–95.
3. Al-Buriahi AK, Al-shaibani MM, Mohamed RM, Al-Gheethi AA, Sharma A, Ismail N. Ciprofloxacin removal from non-clinical environment: a critical review of current methods and future trend prospects. J Water Process Eng. 2022;47: 102725.
4. Olasupo A, Sadiq AC, Suah FB. A novel approach in the removal of ciprofloxacin antibiotic in an aquatic system using polymer inclusion membrane. Environ Technol Innov. 2022;27: 102523.
5. Hamadeen HM, Elkhatib EA. New nanostructured activated biochar for effective removal of antibiotic ciprofloxacin from wastewater: adsorption dynamics and mechanisms. Environ Res. 2022;210: 112929.
6. Roy N, Kannabiran K, Mukherjee A. Studies on photocatalytic removal of antibiotics, ciprofloxacin and sulfamethoxazole, by Fe_3O_4-ZnO-chitosan/alginate nanocomposite in aqueous systems. Adv Powder Technol. 2022;33(8): 103691.
7. Van Thuan D, Nguyen TB, Pham TH, Kim J, Chu TT, Nguyen MV, Nguyen KD, Al-Onazi WA, Elshikh MS. Photodegradation of ciprofloxacin antibiotic in water by using ZnO-doped g-C3N4 photocatalyst. Chemosphere. 2022;308: 136408.
8. Milh H, Yu X, Cabooter D, Dewil R. Degradation of ciprofloxacin using UV-based advanced removal processes: comparison of persulfate-based advanced oxidation and sulfite-based advanced reduction processes. Sci Total Environ. 2021;764: 144510.
9. Li Y, Chen L, Tian X, Lin L, Ding R, Yan W, Zhao F. Functional role of mixed-culture microbe in photocatalysis coupled with biodegradation: total organic carbon removal of ciprofloxacin. Sci Total Environ. 2021;784: 147049.
10. Qalyoubi L, Al-Othman A, Al-Asheh S. Removal of ciprofloxacin antibiotic pollutants from wastewater using nano-composite adsorptive membranes. Environ Res. 2022;215: 114182.
11. El-Bendary N, El-Etriby HK, Mahanna H. Reuse of adsorption residuals for enhancing removal of ciprofloxacin from wastewater. Environ Technol. 2022;43(28):4438–54.
12. Lu D, Xu S, Qiu W, Sun Y, Liu X, Yang J, Ma J. Adsorption and desorption behaviors of antibiotic ciprofloxacin on functionalized spherical MCM-41 for water treatment. J Clean Prod. 2020;264: 121644.
13. Al-Musawi TJ, Mahvi AH, Khatibi AD, Balarak D. Effective adsorption of ciprofloxacin antibiotic using powdered activated carbon magnetized by iron(III) oxide magnetic nanoparticles. J Porous Mater. 2021;28:835–52.
14. Fan H, Ma Y, Wan J, Wang Y, Li Z, Chen Y. Adsorption properties and mechanisms of novel biomaterials from banyan aerial roots via simple modification for ciprofloxacin removal. Sci Total Environ. 2020;708: 134630.
15. Agboola OS, Bello OS. Enhanced adsorption of ciprofloxacin from aqueous solutions using functionalized banana stalk. Biomass Convers Biorefin. 2020. https://doi.org/10.1007/s13399-020-01038-9.
16. Chandrasekaran A, Patra C, Narayanasamy S, Subbiah S. Adsorptive removal of ciprofloxacin and amoxicillin from single and binary aqueous systems using acid-activated carbon from *Prosopis juliflora*. Environ Res. 2020;188: 109825.
17. Yang Y, Zhong Z, Li J, Du H, Li Z. Efficient with low-cost removal and adsorption mechanisms of norfloxacin, ciprofloxacin and ofloxacin on modified thermal kaolin: experimental and theoretical studies. J Hazard Mater. 2022;430: 128500.
18. Antonelli R, Malpass GR, da Silva MG, Vieira MG. Adsorption of ciprofloxacin onto thermally modified bentonite clay: experimental design, characterization, and adsorbent regeneration. J Environ Chem Eng. 2020;8(6): 104553.
19. Mohammed AA, Kareem SL. Enhancement of ciprofloxacin antibiotic removal from aqueous solution using ZnO nanoparticles coated on pistachio shell. Desalin Water Treat. 2021;213:229–39.

20. Langmuir I. The adsorption of gases on plane surfaces of glass, mica and platinum. J Am Chem Soc. 1918;40(9):1361–403.
21. Freundlich HM. Over the adsorption in solution. J Phys chem. 1906;57(385471):1100–7.
22. Johnson RD, Arnold FH. The Temkin isotherm describes heterogeneous protein adsorption. Biochim Biophys Acta Protein Struct Mol Enzymol. 1995;1247(2):293–7.
23. Lagergren SK. About the theory of so-called adsorption of soluble substances. Sven Vetenskapsakad Handingarl. 1898;24:1–39.
24. Ho YS, McKay G. Pseudo-second order model for sorption processes. Process Biochem. 1999;34(5):451–65.
25. Kumar PS, Ramalingam S, Sathyaselvabala V, Kirupha SD, Murugesan A, Sivanesan S. Removal of cadmium(II) from aqueous solution by agricultural waste cashew nut shell. Korean J Chem Eng. 2012;29:756–68.
26. Bezerra MA, Santelli RE, Oliveira EP, Villar LS, Escaleira LA. Response surface methodology (RSM) as a tool for optimization in analytical chemistry. Talanta. 2008;76(5):965–77.
27. Ferreira SC, Bruns RE, Ferreira HS, Matos GD, David JM, Brandão GC, da Silva EP, Portugal LA, Dos Reis PS, Souza AS, Dos Santos WN. Box-Behnken design: an alternative for the optimization of analytical methods. Anal Chim Acta. 2007;597(2):179–86.
28. Hashem A, Sanousy MA, Mohamed LA, Okoye PU, Hameed BH. Natural and low-cost *P. turgidum* for efficient adsorption of Hg(II) ions from contaminated solution: isotherms and kinetics studies. J Polym Environ. 2021;29:304–12.
29. Aslan NE, Cebeci YA. Application of Box-Behnken design and response surface methodology for modeling of some Turkish coals. Fuel. 2007;86(1–2):90–7.
30. Zhang TF, Yang JF, Lin DK. Small box–Behnken design. Stat Probab Lett. 2011;81(8):1027–33.
31. St L, Wold S. Analysis of variance (ANOVA). Chemometr Intell Lab Syst. 1989;6(4):259–72.
32. Kim TK. Understanding one-way ANOVA using conceptual figures. Korean J Anesthesiol. 2017;70(1):22–6.
33. Singh K, Gautam M, Chandra B, Kumar A. Removal of Pb(II) from its aqueous solution by activated carbon derived from Balam Khira (*Kigelia Africana*). Desalin Water Treat. 2016;57(51):24487–97.